Solution Structure of Methionine-Oxidized Amyloid β-Peptide (1−40). Does Oxidation Affect Conformational Switching?[†,‡]

Andrew A. Watson, David P. Fairlie,* and David J. Craik*

Centre for Drug Design and Development, The University of Queensland, Brisbane QLD 4072, Australia

Received May 11, 1998; Revised Manuscript Received July 13, 1998

ABSTRACT: The solution structure of Aβ(1−40)Met(O), the methionine-oxidized form of amyloid β-peptide Aβ(1−40), has been investigated by CD and NMR spectroscopy. Oxidation of Met35 may have implications in the aetiology of Alzheimer's disease. Circular dichroism experiments showed that whereas Aβ(1−40) and Aβ(1−40)Met(O) both adopt essentially random coil structures in water (pH 4) at micromolar concentrations, the former aggregates within several days while the latter is stable for at least 7 days under these conditions. This remarkable difference led us to determine the solution structure of Aβ(1−40)Met(O) using ^{1}H NMR spectroscopy. In a water−SDS micelle medium needed to solubilize both peptides at the millimolar concentrations required to measure NMR spectra, chemical shift and NOE data for Aβ(1−40)Met(O) strongly suggest the presence of a helical region between residues 16 and 24. This is supported by slow H−D exchange of amide protons in this region and by structure calculations using simulated annealing with the program XPLOR. The remainder of the structure is relatively disordered. Our previously reported NMR data for Aβ(1−40) in the same solvent shows that helices are present over residues 15−24 (helix 1) and 28−36 (helix 2). Oxidation of Met35 thus causes a local and selective disruption of helix 2. In addition to this helix−coil rearrangement in aqueous micelles, the CD data show that oxidation inhibits a coil-to-β-sheet transition in water. These significant structural rearrangements in the C-terminal region of Aβ may be important clues to the chemistry and biology of Aβ(1−40) and Aβ(1−42).

The underlying aetiology of Alzheimer's disease (AD)[1] is unknown. One theory is that AD is the result of oxidative stress (*1*) associated with inflammation in the brain, generating noxious free radicals and reactive oxygen species that cause cellular damage (*2*). The 39−43 residue amyloid β-peptide (Aβ), which is known to produce free radicals and induce hydrogen peroxide production in clonal cell lines (*2*−*8*), is present as the major component of the neuritic plaques that are diagnostic for AD (*9*). The mechanism for Aβ-associated radical production and inducement of hydrogen peroxide production is unknown. Methionine 35 of Aβ is the most susceptible residue to oxidation in vitro, undergoing preferential oxidation to the methionine sulfoxide [Met(O)], and this is also likely in vivo under conditions of oxidative stress (*10*).

A number of studies have been focused on possible roles of Met35 in AD, particularly its influence in small fragments of Aβ on aggregation, fibril formation, radical formation, and cellular toxicity. The peptide Aβ(25−35) shows some of the same biological properties as full-length Aβ, including the formation of fibrils (*11*), free radicals, and neurotoxicity (*4*). Residues 33−35 are thought to be particularly crucial for aggregation and neurotoxicity of Aβ peptides (*11*). Oxidation of Met35 to methionine sulfoxide in the fragment Aβ(25−35) can be arrested by a radical scavenger (*5*), and Met35 is proposed to be a key residue for Aβ radicalization, aggregation, and neurotoxicity (*4*). While low concentrations of Aβ(25−35) (10 nM) and the mutant Aβ(25−35)M35L ($\geq$1 μM) inhibit lipid peroxidation (*12*), the former (but not the latter) has been found to stimulate lipid peroxidation with oxidation of methionine at higher concentrations ($\geq$100 μM).

However, substitution of Met35 (*11*) in Aβ(25−35) by Asp, Ala (*13*), Ser, and Cys still results in aggregation and neurotoxicity, suggesting that this residue is not essential for these properties (*2*). The mutants of M35S and M35E in Aβ(1−42) are reported (*14*) to cause cellular toxicity similar to, but fiber morphology different from, that of Aβ(1−42), while the M35Nle mutant forms neurotoxic aggregates that are smaller or less stable (*11*). Lorenzo et al. (*15*) claim that oxidation is not required for aggregation or neurotoxicity of Aβ(1−40), and Esler et al. (*16*) report that no significant oxidation of peptides occurred in studies of deposition of Aβ(1−40) or Aβ(10−35)NH_2 onto AD plaques. Some of

[†] This work was supported by the National Health and Medical Research Council of Australia. D.J.C. is an Australian Research Council Senior Fellow.

[‡] Coordinates have been deposited in the Brookhaven Protein Data Bank under ID code 1ba6.

* To whom correspondence should be addressed (D.J.C.: fax, +61-7-3365-2487; e-mail, d.craik@mailbox.uq.edu.au; DPF: fax, +61-7-3365-1990; e-mail, d.fairlie@mailbox.uq.edu.au).

[1] Abbreviations: Aβ, amyloid β-peptide; Met(O), methionine sulfoxide; APP, amyloid precursor protein; NMR, nuclear magnetic resonance; SDS, sodium dodecyl sulfate; AD, Alzheimer's disease; TFA, trifluoroacetic acid; HPLC, high-performance liquid chromatography; ESMS, electrospray mass spectrum; TOCSY, total correlation spectroscopy; NOESY, nuclear Overhauser enhancement spectroscopy; CD, circular dichroism; rmsd, root-mean-square deviation.

S0006-2960(98)01075-7 CCC: $15.00
Published on Web 08/22/1998

these results cast some doubt on the importance of Met35 in AD and about a redox role for Met35.

Recently, Seilheimer et al. (*14*) reported an extensive study of a range of Aβ peptides, some containing the methionine sulfoxide, in which there were distinct morphological changes associated with the formation of mature fibrils from monomeric Aβ and there was a strong correlation between the Aβ sequence, aggregation rate, fiber morphology, density of fibers, and biological effect. Aβ(1−40) and its oxidized form Aβ(1−40)Met(O) had low propensities to aggregate to mature fibrils and low cellular toxicity, consistent with other reports that Aβ(1−40) has a low propensity for fibrilgenesis (*17*). In contrast, Aβ(1−42) and Aβ(1−42)-Met(O) showed higher rates of fiber formation which correlated well with higher rates of aggregation and higher cellular toxicity. Aβ fibrils are characterized by an antiparallel β-pleated sheet conformational structure compared with the random coil conformation of freshly generated monomeric Aβ. Increased production of Aβ(1−42) is implicated in the early onset familial forms of AD (*18*) and is the main form of Aβ found in neuritic plaques.

Despite the many structural studies on fragments of Aβ peptides, firm conclusions are only now emerging about the structural identity of the longer (39−43 residue) Aβ peptides in aqueous, lipidic, and other solutions. Our recent NMR study of Aβ(1−40) in aqueous SDS micelles (*19*), used to simulate a water−membrane interface, has shown that this peptide is helical between residues 15 and 36 with a kink in the helix around residues 25−27. Consistent with this result, Aβ(1−40) is reported to be helical between residues 15 and 23, and 31 and 35, in TFE/H_2O solution (*20*). The helical region is essentially the hydrophobic domain of Aβ thought to be the transmembrane region of the amyloid precursor protein, although recent results (*21*) suggest that the transmembrane domain of APP could be in a location slightly different from that which is commonly accepted (*22*). Terzi et al. (*23*) recently reported that the mode of interaction of Aβ(1−40) with model lipid membrane systems is different from that found for micelles. Positively charged residues of Aβ(1−40) are proposed to interact electrostatically with a negatively charged lipid bilayer, without penetration of the bilayer, to induce helicity.

On the basis of the fact that Aβ peptide ultimately finds its way into the plaques that characterize AD, that some of the plaque-containing peptide is the oxidized peptide Aβ-(1−40)Met(O), that peroxide is evidently formed in the vicinity of Aβ, and that oxidation of Met35 is reported to be associated with AD, we have investigated the structural consequences of this oxidation reaction for Aβ(1−40). Here we use CD and NMR spectroscopy to study the structure of the methionine-oxidized form, Aβ(1−40)Met(O), in the same micelle−water environment for which we have previously determined the structure of Aβ(1−40) (*19*).

MATERIALS AND METHODS

Trifluoroacetic acid (TFA) was purchased from Auspep (Melbourne, Australia) and acetonitrile (HPLC grade) from BDH (Poole, England). Other chemicals and solvents were of reagent grade. Electrospray mass spectra were recorded on a Perkin-Elmer SCIEX API III triple-quadrupole mass spectrometer. Preparative reverse phase HPLC was performed on a Waters Delta-Pak PrepPak C_{18} 40 mm × 100 mm cartridge (100 Å) using a Waters Delta Prep 4000 preparative chromatography system with a solvent system of A (water/0.1% TFA) and B (90% acetonitrile/0.1% TFA) and a linear gradient from 0 to 100% B over 50 min. Analytical runs were performed similarly but on a Waters Delta-Pak Radial-Pak C_{18} 8 mm × 100 mm cartridge. Elution profiles were monitored at 214 nm.

Preparation of Aβ(1−40)Met(O). Aβ(1−40)Met(O) was obtained by oxidation of Aβ(1−40) with hydrogen peroxide. Aβ(1−40) (10 mg), synthesized manually by solid phase peptide synthesis as previously described (*19*), was dissolved in aqueous hydrogen peroxide (3% w/w, 2 mL) and the mixture stirred at 293 K for 4 h. The oxidized product was purified by RP-HPLC and stored as a lyophilized white powder. Aβ(1−40)Met(O) elutes ∼2 min earlier than Aβ-(1−40) by reverse phase HPLC. ESMS $(MH)^+$: calcd for $C_{194}H_{296}N_{53}O_{59}S$ 4346.9, found 4346.2.

CD Spectra. Circular dichroism measurements were made on a JASCO 710 spectropolarimeter equipped with a thermostatable cell holder using a 0.1 mm path length JASCO quartz cell with a 300 μL capacity. The peptide (0.05 mg) was dissolved in either water (pH 4) or aqueous SDS micelles (100 mM, pH 6) at 294 K. Peptide concentrations were determined by quantitative amino acid analysis [PICO-Tag method (*24*)]. Ellipticity was calibrated using (1*S*)-(+)-10-camphorsulfonic acid. $[\theta]$ is the mean residue molar ellipticity calculated from $[\theta] = \theta(\mathrm{MWR}/10lc)$, where θ is the ellipticity in millidegrees, MWR is the molecular weight of the peptide divided by the number of residues, c is the sample concentration (milligrams per milliliter), and l is the cell path length in centimeters. CD spectra were smoothed using a noise reduction option. The percent helicity was calculated from molar ellipticities at 222 nm (*25*−*27*).

NMR Experiments. For NMR studies, Aβ(1−40)Met(O) was dissolved in 0.55 mL of 100 mM sodium dodecyl-d_{25} sulfate in either 90% H_2O/10% D_2O or 100% D_2O (pH 5.3) to give a final concentration of 1 mM. To aid dissolution, the sample was sonicated for 10 s. ^{1}H NMR spectra of Aβ-(1−40)Met(O) were acquired at 500 and 750 MHz on Bruker AMX-500 and DRX-750 spectrometers, respectively. NOESY (*28*) and TOCSY (*29*) spectra were acquired at 298 K. Spectra were acquired in the phase-sensitive mode using time-proportional phase incrementation for quadrature detection in the t_1 dimension (*30*).

The solvent signal was suppressed either by low-power presaturation during the relaxation delay or by the use of pulsed field gradients (*31*). NOESY data were collected with mixing times of 100 and 150 ms. The rate of disappearance of amide protons signals on dissolution of the peptide in SDS/D_2O (pH 5.3) was measured from a series of one-dimensional (1D) spectra recorded from 5 to 50 min after dissolution.

Spectral data were processed on a Silicon Graphics Indy computer using standard Bruker software (XWINNMR, version 1.2). Data were zero-filled to 4096 points in F_2 and to 2048 points in F_1 and then transformed with a sine-bell-squared window function shifted by between $\pi/2$ and $\pi/4$ as appropriate. Polynomial baseline correction was carried out on either side of the residual water signal. Spectra were referenced for the SDS/aqueous solutions to the HDO peak according to the method of Wishart et al. (*32*).

Structure Calculations. The 100 ms NOESY spectrum of Aβ(1−40)Met(O) in H_2O/SDS solution (750 MHz, 298 K, pH 5.3) was used for extraction of distance restraints used in quantitative structure calculations. All cross-peaks which could be assigned unambiguously were classified according to their intensity. Three categories were defined, strong, medium, or weak, which resulted in restraints on the upper limit of proton separations of 2.7, 3.5, and 5.0 Å, respectively, with allowances for the use of pseudoatoms where appropriate. Hydrogen bond distance restraints were also included for amide protons which exchanged slowly in D_2O and where a hydrogen bond acceptor had been consistently predicted in preliminary structure calculations in the absence of hydrogen bond restraints. In these cases, i.e., 16(O)−20(HN), 18(O)−22(HN), and 19(O)−23(HN), the distance between the amide proton and the receptor carbonyl oxygen was restrained to 1.58−2.30 Å and that between the amide nitrogen and the carbonyl oxygen to 1.58−3.20 Å.

Fifty structure calculations were carried out in XPLOR (*33*) using simulated annealing using standard XPLOR potential wells and force constants. A modified version of the standard XPLOR topology file with a methionine sulfoxide residue was produced. The sulfur stereocenter had the *R* configuration. Simulated annealing calculations were carried out using the protocol sa.inp (30 ps of dynamics at 2000 K followed by 16 ps of dynamics during which the system was cooled linearly to 50 K). The structures were subjected to a further period of simulated annealing with emphasis on experimental constraints (16 ps of dynamics with a temperature ramp from 1000 to 50 K) and then minimized (4000 cycles) using the Powell algorithm. The calculated structures were examined visually using the InsightII molecular graphics program of Biosym/MSI.

RESULTS

The oxidized form of Aβ(1−40), namely Aβ(1-40)Met-(O), is more polar than Aβ(1-40) and soluble at low millimolar concentrations in both water [unlike Aβ(1-40)] and SDS micelles (100 mM). Preliminary circular dichroism spectra were used to compare the structures of Aβ(1−40)-Met(O) and Aβ(1−40) in these solvents. In water (pH 4), Aβ(1−40)Met(O) exists as a random coil structure (Figure 1a) that persists for many days and shows little propensity to adopt the β-sheet structure typical of aggregated Aβ peptides. On the other hand, the unoxidized Aβ(1−40) initially produces a CD spectrum characteristic of a random coil, but this changes over several days (Figure 1b) to that of a β-sheet structure that is associated with aggregation and fibril formation. This remarkable contrast prompted us to investigate in more detail structural differences between the two peptides and address the question of why oxidation retards β-sheet formation. By CD, both peptides have a significant helical content in aqueous SDS micelles (Figure 1c,d), but there is a significant reduction in helicity upon oxidation [37% Aβ(1−40) vs 29% Aβ(1−40)Met(O)].

NMR studies were undertaken to determine the precise location of helical region(s) in Aβ(1−40)Met(O) and to identify how oxidation of the thioether side chain of methionine affects conformation. Oxidation of Met35 has a number of potential structural and/or electronic consequences. Methionine sulfoxide is sterically bulkier than

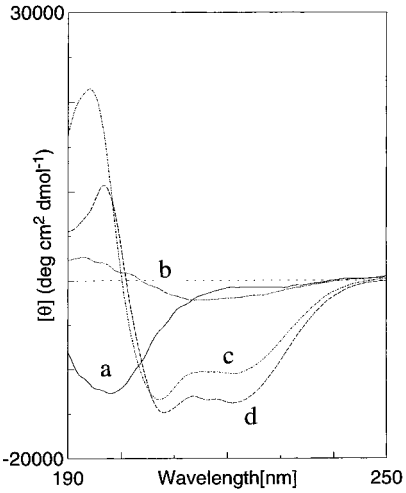

FIGURE 1: CD spectra of Aβ peptides: (a) Aβ(1−40)Met(O) and (b) Aβ(1−40) in water (pH 4) after 7 days and (c) Aβ(1−40)-Met(O) and (d) Aβ(1−40) in SDS micelles (100 mM, pH 6).

Scheme 1

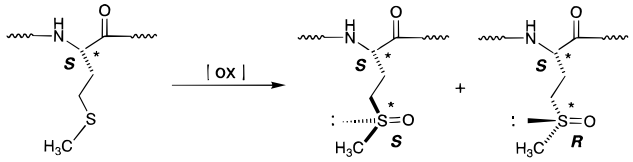

methionine and has a greater potential to act as a hydrogen bond acceptor of a main chain amide NH proton. Oxidation not only results in a marked change in the polarity of the methionine residue itself but also is known to have a significant effect on the overall polarity of a number of proteins (*10*, *34*). For Aβ(1−40)Met(O), this is reflected in a marked decrease in the HPLC retention time compared to that of Aβ(1−40).

An additional consequence of oxidation of Met35 is the generation of a new stereogenic center at the sulfur atom, resulting in two diastereomers of Aβ(1−40)Met(O) as indicated in Scheme 1 each with different hydrogen bonding potentials. In principle, the presence of diastereomers can be detected by NMR spectroscopy.

To compare in more detail the structure of Aβ(1−40)-Met(O) with its unoxidized form, it was necessary to examine it under conditions where Aβ(1−40) is also soluble and not prone to aggregation. NMR structure determinations require millimolar concentrations for detection, so we examined Aβ-(1−40)Met(O) in aqueous SDS micelles, a water−lipid like environment that may simulate the water−membrane environment encountered by Aβ(1−40) when incorporated in its membrane-spanning polypeptide precursor (amyloid precursor protein). The sample was stable for several months at room temperature in this solvent and not prone to aggregation.

NMR data for Aβ(1−40)Met(O) dissolved in SDS micelles were collected at 298 K and pH 5.3. The spectra were assigned using the sequential assignment technique (*35*). Figure 2, which shows a 750 MHz NOESY spectrum of Aβ-(1−40)Met(O) in aqueous SDS micelles, indicates sequential assignments for all residues. The pattern of cross-peaks in this fingerprint region of the NOESY spectrum is similar to that for Aβ(1−40), with all of the differences being confined to residues close to Met35 in the sequence. The two

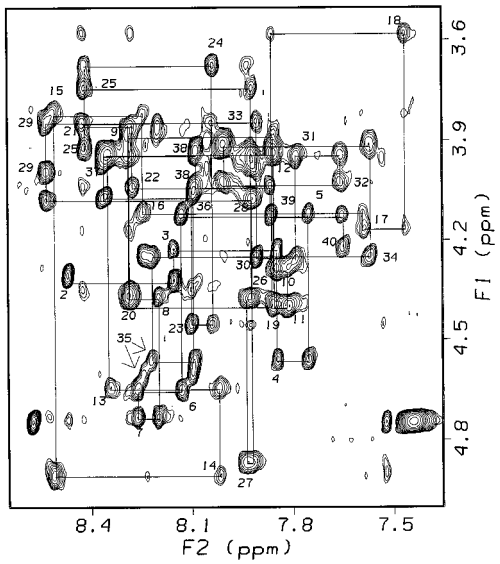

FIGURE 2: αH−NH region of a NOESY spectrum (100 ms, 750 MHz) of Aβ(1−40)Met(O) in SDS micelles (100 mM) at 298 K and pH 5.3. The sequential assignment is indicated with the intraresidue cross-peaks numbered.

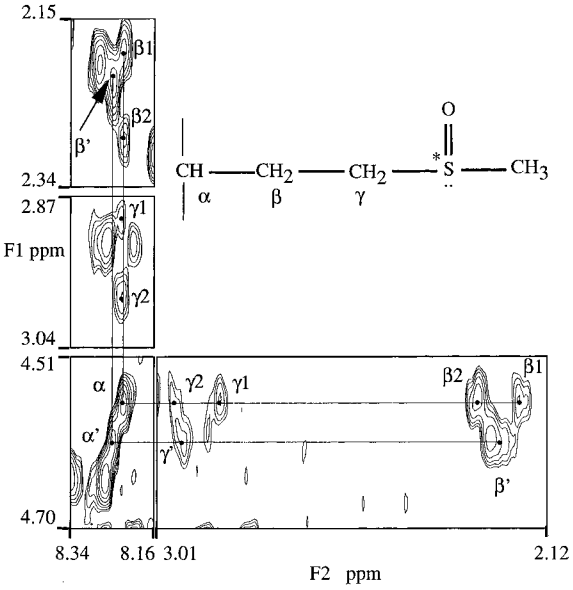

FIGURE 3: Expanded region of the NOESY spectrum of Aβ(1−40)Met(O) (100 ms, 750 MHz) illustrating two sets of resonances for diastereomers of the methionine sulfoxide residue.

diastereomers for the methionine sulfoxide protons are indicated by two sets of resonances (α-NH cross-peaks at 4.60 and 8.25, and 4.56 and 8.22, ppm), as illustrated in Figure 3. Although it was not possible to determine which of the two sets of complementary resonances corresponds to which absolute configuration at the sulfur atom, it is interesting that the β-protons are clearly nondegenerate for one of the diastereomers but are overlayed for the other. Figure 4 shows the assigned NH−NH region of the spectrum and illustrates a significant number of sequential NH−NH contacts. These provide a strong preliminary indication of at least some regions of helicity within the structure.

Shown in Figure 5 are the differences between measured α-proton chemical shifts and random coil values (*36*) for each residue of Aβ(1−40)Met(O). Deviations of more than −0.1 ppm from random coil for several successive residues

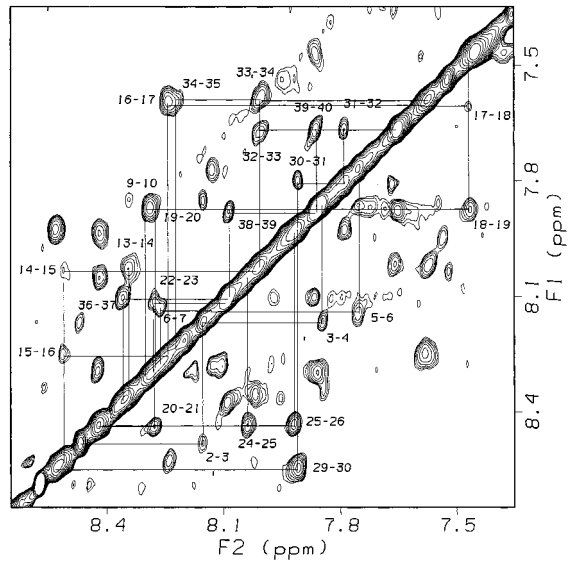

FIGURE 4: NH−NH region of the NOESY spectrum of Aβ(1−40)Met(O) (100 ms, 750 MHz) at 298 K and pH 5.3. Sequential connectivities are indicated.

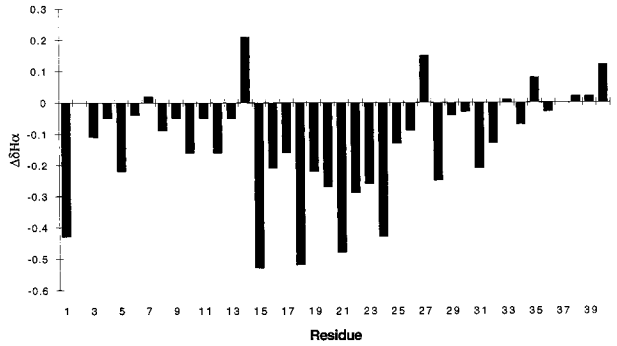

FIGURE 5: Differences of α-proton chemical shifts from random coil values for Aβ(1−40)Met(O). The random coil value for methionine was used for methionine sulfoxide.

are usually associated with helical structures. The data in Figure 5 suggest helicity between residues 15 and 25 of Aβ(1−40)Met(O), and these data are similar for this region to the data previously reported for Aβ(1−40) under the same conditions (*19*). However, there are also significant differences between Aβ(1−40)Met(O) and Aβ(1−40) in C-terminal residues 33−40, possibly reflecting disruption of structure in this region for Aβ(1−40)Met(O).

D_2O exchange experiments revealed two regions of slow exchanging amide protons, residues 17−24 and 30−34, although there is overlap in the latter region. These data support a helix between 17 and 24 and a smaller structured region from residues 30 to 32. The kinked region found in the Aβ(1−40) structure at residues 25−27 also is supported for Aβ(1−40)Met(O) by fast D_2O exchange of their amide protons, by the lack of i,i+3 connectivities in this region, and by a large positive $\Delta H\alpha$ for N27.

Analysis of the NOESY spectra provided 205 intraresidue, 102 sequential, and 33 medium-range connectivities that are summarized in Figure 6. Helical structure is supported by a number of $\alpha\beta(i,i+3)$ and αHN$(i,i+3)$ connectivities between residues 17 and 25. However, C-terminal helix 2 (residues 28−36) found for Aβ(1−40) is clearly not as well defined for Aβ(1−40)Met(O). The absence of key i,i+3 contacts through residues 33−36 [e.g., αHN$(i,i+3)$ for

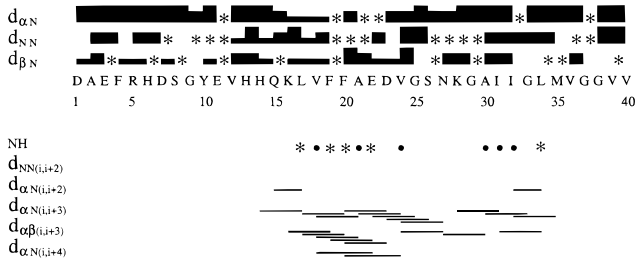

FIGURE 6: NOE connectivities observed for Aβ(1−40)Met(O) in SDS micelles (298 K, pH 5.3). Asterisks represent ambiguity due to overlap. Slow D_2O exchangeable protons are represented by solid circles or asterisks. In the latter case, the assignment of slow exchanging peaks was ambiguous due to overlap of several protons, but the proposed assignments are consistent with those found for Aβ(1−40).

residues 32−35 and 34−37] that were present for Aβ(1−40) (*19*) reflects disruption of helicity in this region due to Met(O)35.

Structure Calculations. Fifty structures were generated using simulated annealing and energy minimization protocols incorporating distance restraints based on the NOESY data. No dihedral constraints were used in the calculations due to the broadness of resonances and the lack of satisfactory COSY data. Ten structures were selected on the basis of low energy and violations. None of the structures had more than three distance violations of >0.3 Å. Figure 7 shows an overlay of the structures superimposed through the backbone region of residues 16−24. The average pairwise backbone rmsd value for the superimposed structures over residues 16−24 is 0.28 Å. The main structural feature is an α-helix spanning residues 16−24. The rest of the peptide appears to be disordered with poor superimposition in other regions, including the second helical region (residues 28−36, rmsd of 2.2 Å) found for Aβ(1−40).

DISCUSSION

Methionine is one of the most readily oxidized amino acid constituents of proteins. A variety of oxidizing agents are available in biological systems that can affect this oxidation, including reactive oxygen species (*10*). In this investigation, we observe a conformational change in Aβ(1−40) as a result of oxidation of a methionine residue to its diastereomeric sulfoxide.

The structure of Aβ(1−40) is concentration- and solvent-dependent. This and other CD studies have shown that Aβ-(1−40) in water exists in equilibrium between random coil and β-sheet structures at concentrations below 100 μM. At higher concentrations (ca. 200 μM), a β-sheet structure predominates (*37*). Higher solubility is observed in aqueous TFE or SDS micelles, with an α-helical structure predominating in these solvents at the millimolar peptide concentrations needed to conduct NMR studies (*19*, *20*).

By contrast with Aβ(1−40), we find here that the more water soluble Aβ(1−40)Met(O) (soluble at millimolar concentrations) is mainly a random coil in water (pH 4) at micromolar concentrations used for CD studies, and there is no evidence of aggregation or precipitation after 7 days. There have been several conflicting reports of the structural and physicochemical properties of this oxidized peptide. Seilheimer et al. (*14*) report that Aβ(1−40)Met(O) shows a prolonged lag time before conversion from a random coil to a β-sheet structure, while Snyder et al. (*38*) claim that Aβ-(1−40)Met(O) has an enhanced rate of aggregation compared with unoxidized Aβ(1−40). The latter report is in conflict with our results but may be the result of different solution conditions. In Aβ(1−42)Met(O), the conformational change from random coil to β-sheet evidently occurs quickly, highlighting the impact that residues Ile41 and Ala42 have on the physical properties of Aβ (*14*). Aβ(1−42) is proposed to play a key role in seeding the formation of neuritic plaques and is more amyloidogenic and less soluble than Aβ(1−40) (*17*). A number of early onset familial forms of AD are attributed to higher production levels of Aβ(1−42) (*18*).

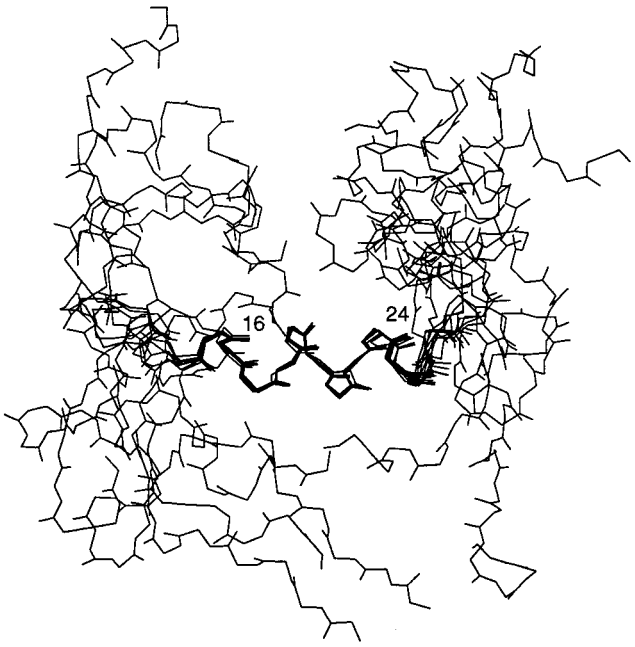

FIGURE 7: Overlay of 10 low-energy structures of Aβ(1−40)Met-(O) superimposed on the backbone of residues 16−24.

In SDS micelles, Aβ(1−40)Met(O) has been shown here to adopt a partial helical structure. The CD results show decreased helix content for Aβ(1−40)Met(O) versus Aβ-(1−40), and this is strongly supported by NMR results which indicate that while both peptides adopt a helix between residues ca. 16−24, the helix between residues 28−36 that is observed for Aβ(1−40) is not well-defined in the oxidized peptide Aβ(1−40)Met(O). We conclude that oxidation at Met35 destabilizes this second helix.

A helical wheel model for residues 17−40 of Aβ(1−40) would place residues on four surfaces (F20, V24, K28, I32, V36, and V40 on face 1, F19, D23, N27, I31, M35, and V39 on face 2, L17, A21, G25, G29, G33, and G37 on face 3, and V18, E22, S26, A30, L34, and G38 on face 4). Although the C-terminal half of Aβ(1−40) is essentially helical in SDS micelles and TFE, the conformation also expected in a membrane, two of these surfaces are dominated by bulky hydrophobic branched residues (Val and Ile) or glycine residues which have intrinsic preferences for β-sheet conformations. It is therefore not surprising that the peptide loses its helicity in water.

The distinctive stretch of glycine residues with *i*,*i*+4 spacing between residues 25 and 37 creates a groove which exposes the backbone on face 3 of the helix. The relatively high exposure of the backbone hydrogen bonds in this region may facilitate unwinding of helix 2 (GAIIGLMV) under

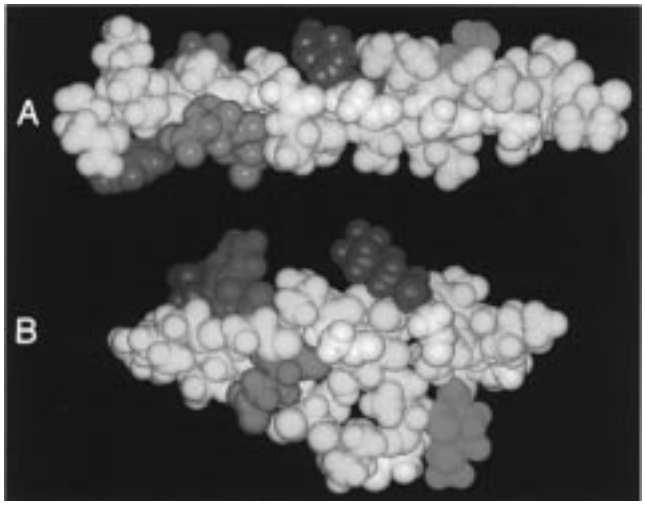

FIGURE 8: Comparison of residues 15−40 for the lowest-energy structures of (A) Aβ(1−40) and (B) Aβ(1−40)Met(O). The colors refer to the following residues: white, Gly; red, Glu and Asp; blue, Lys; green, Met or Met(O); violet, Phe; and yellow, other residues. Residues after position 25 in Aβ(1−40)Met(O) are not well-defined. Although the lowest-energy structure is shown in panel B for purposes of illustration, all calculated structures for Aβ(1−40)-Met(O) show a similar disruption of the glycine groove seen in panel A for Aβ(1−40).

certain solution conditions or when triggered by the presence of the polar sulfoxide side chain upon oxidation of Met35. Figure 8A shows the remarkable groove in helix 2 in the solution NMR structure of Aβ(1−40) (*19*) (PDB code 1ba4) and illustrates the proximity of Met35 to this groove. Durell et al. (*39*) have noted the presence of this groove in putative ion channel models of Aβ, and its functional significance may be multifaceted. By contrast, the solution structures for Aβ(1−40)Met(O) calculated here show that this groove is completely disrupted upon oxidation of Met35 (Figure 8B).

Redox-induced structural changes triggered by oxidation of methionine, as found here for oxidation of Met35 in Aβ-(1−40), have previously been identified for aggregating peptides (*40*) with oxidation to either the sulfoxide or sulfone causing a conformational transition from α-helix to β-strand. Also, the dimerization property of a designed leucine zipper peptide is abolished upon oxidation of a single methionine to its sulfoxide (*41*). Changes in the function of proteins as a result of oxidation and/or reduction of methionine have been proposed as one means of homeostasis control in biological systems (*10*). Aβ(1−40) appears to be a conformationally fragile peptide which exists in a finely balanced equilibrium represented by helix ↔ random coil ↔ β-sheet. The well-established precedent of methionine oxidation as a conformational trigger in other peptides may also be important for Aβ.

In reports of structure−activity studies on Aβ(25−35) and Aβ(1−42), Pike et al. (*11*) found that a β-turn at residues 25−28 and a hydrophobic domain at residues 29−35 were essential for aggregation, these regions being identified by our NMR studies as a helix break and a helix, respectively, in Aβ(1−40). For Aβ(25−35), mutations I31L, I32L, and G33A greatly reduced aggregation and neurotoxicity, suggesting an important packing role for these side chain residues in aggregation. Unfortunately, these mutations were not examined in Aβ(1−42). Interestingly, substitution in Aβ-(25−35) of Met35 with Leu, Nle, Lys, or Tyr prevented detectable aggregation, suggesting that hydrophobicity and/or size alone of the side chain are insufficient for aggregation. This result is consistent with the reduced aggregation for Aβ(1−40) upon methionine oxidation being the result of hydrogen bonding or entropic destabilization rather than a simple steric packing phenomenon.

In summary, Aβ(1−40) is thought to rearrange from its helical conformation present within the membrane-spanning APPs, to a random coil form in water, to a β-sheet structure which aggregates and precipitates. Our studies suggest that oxidation of Met35 in Aβ(1−40) destabilizes the helical form, but also hinders a conformational transition from random coil to β-sheet. Oxidation thus reduces the propensity of the peptide to aggregate to form fibrils (*14*). However, this property does not evidently extend to Aβ(1−42)Met(O) (*14*), suggesting that the capacity of Met(O) to retard aggregation is overcome by the influence of residues 41 and 42. We do not know whether the oxidative generation of a stereogenic center at the sulfur atom of Met35, and the resulting formation of diastereomers, also affects the aggregating tendency of Aβ(1−40)Met(O).

ACKNOWLEDGMENT

We thank Trudy Bond for amino acid analysis.

SUPPORTING INFORMATION AVAILABLE

Table of ^{1}H NMR chemical shifts for Aβ(1−40)Met(O) in SDS micelles at 298 K, pH 5.3, and 750 MHz (2 pages). Ordering information is given on any current masthead page.

REFERENCES

1. Markesbery, W. R. (1997) *Free Radical Biol. Med. 23*, 134−147.
2. Kay, C. J. (1997) *FEBS Lett. 403*, 230−235.
3. Behl, C., Davis, J. B., Lesley, R., and Schubert, D. (1994) *Cell 77*, 817−822.
4. Hensley, K., Carney, J. M., Mattson, M. P., Aksenova, M., Harris, M., Wu, J. F., Floyd, R. A., and Butterfield, D. A. (1994) *Proc. Natl. Acad. Sci. U.S.A. 91*, 3270−3274.
5. Hensley, K., Aksenova, M., Carney, J. M., Harris, M., and Butterfield, D. A. (1995) *NeuroReport 6*, 489−492.
6. Harris, M. E., Carney, J. M., Cole, P. S., Hensley, K., Howard, B. J., Martin, L., Bummer, P., Wang, Y., Pedigo, N. W., Jr., and Butterfield, D. A. (1995) *NeuroReport 6*, 1875−1879.
7. Butterfield, D. A., Martin, L., Carney, J. M., and Hensley, K. (1996) *Life Sci. 58*, 217−228.
8. Kelly, J. F., Furukawa, K., Barger, S. W., Rengen, M. R., Mark, R. J., Blanc, E. M., Roth, G. S., and Mattson, M. P. (1996) *Proc. Natl. Acad. Sci. U.S.A. 93*, 6753−6758.
9. John, V., Latimer, L. H., Tung, J. S., and Dappen, M. S. (1997) *Annu. Rep. Med. Chem. 32*, 11−20.
10. Vogt, W. (1995) *Free Radical Biol. Med. 18*, 93−105.
11. Pike, C. J., Walencewicz-Wasserman, A. J., Kosmoski, J., Cribbs, D. H., Glabe, C. G., and Cotman, C. W. (1995) *J. Neurochem. 64*, 253−265.
12. Walter, M. F., Mason, P. E., and Mason, R. P. (1997) *Biochem. Biophys. Res. Commun. 233*, 760−764.
13. Sato, K., Wakamiya, A., Maeda, T., Noguchi, K., Takashima, A., and Imahori, K. (1995) *J. Biochem. 118*, 1108−1111.
14. Seilheimer, B., Bohrmann, B., Bondolfi, L., Müller, F., Stüber, D., and Döbeli, H. (1997) *J. Struct. Biol. 119*, 59−71.
15. Lorenzo, A., Matsudaira, P., and Yankner, B. A. (1993) *Soc. Neurosci. Abstr. 19*, 184.
16. Esler, W. P., Stimson, E. R., Ghilardi, J. R., Lu, Y.-A., Felix, A. M., Vinters, H. V., Mantyh, P. W., Lee, J. P., and Maggio, J. E. (1996) *Biochemistry 35*, 13914−13921.

17. Jarrett, J. T., Berger, E. P., and Lansbury, P. T., Jr. (1993) *Biochemistry 32*, 4693−4697.
18. Hendricks, L., and Van Broeckhoven, C. (1996) *Eur. J. Biochem. 237*, 6−15.
19. Coles, M., Bicknell, W., Watson, A. A., Fairlie, D. P., and Craik, D. J. (1998) *Biochemistry 37*, 11064−11077.
20. Sticht, H., Bayer, P., Willbold, D., Dames, S., Hilbich, C., Beyreuther, K., Frank, R. W., and Rösch, P. (1995) *Eur. J. Biochem. 233*, 293−298.
21. Tischer, E., and Cordell, B. (1996) *J. Biol. Chem. 271*, 21914−21919.
22. Kang, J., Lemaire, H.-G., Unterbeck, A., Salbaum, J. M., Masters, C. L., Grzeschik, K.-H., Multhaup, G., Beyreuther, K., and Müller-Hill, B. (1987) *Nature 325*, 733−736.
23. Terzi, E., Hölzemann, G., and Seelig, J. (1997) *Biochemistry 36*, 14845−14852.
24. PICO-Tag Amino Acid Analysis System, Waters Associates Operators Manual (number 88140) (1984) Waters Associates, Milford, MA.
25. Benson, D. R., Hart, B. R., Zhu, X., and Doughty, M. B. (1995) *J. Am. Chem. Soc. 117*, 8502−8510.
26. Chang, C. T., Wu, C.-S. C., and Yang, J. T. (1978) *Anal. Biochem. 91*, 13−31.
27. Lyu, P. C., Sherman, J. C., Chen, A., and Kallenbach, N. R. (1991) *Proc. Natl. Acad. Sci. U.S.A. 88*, 5317−5320.
28. Jeener, J., Meier, B. H., Bachmann, P., and Ernst, R. R. (1979) *J. Chem. Phys. 71*, 4546−4553.
29. Braünschweiler, L., and Ernst, R. R. (1983) *J. Magn. Reson. 53*, 521−528.
30. Marion, D., and Wüthrich, K. (1983) *Biochem. Biophys. Res. Commun. 113*, 967−974.
31. Piotto, M., Saudek, V., and Sklenar, V. (1992) *J. Biomol. NMR 2*, 661−665.
32. Wishart, D. S., Bigam, C. G., Yao, J., Abildgaard, F., Dyson, H. J., Oldfield, E., Markley, J. L., and Sykes, B. D. (1995) *J. Biomol. NMR 6*, 135−140.
33. Brünger, A. T. (1992) *XPLOR version 3.0 Manual*, Yale University Press, New Haven, CT.
34. Chao, C.-C., Ma, Y.-S., and Stadtman, E. (1997) *Proc. Natl. Acad. Sci. U.S.A. 94*, 2969−2974.
35. Wüthrich, K. (1986) *NMR of Proteins and Nucleic Acids*, Wiley, New York.
36. Wishart, D. S., Bigam, C. G., Holm, A., Hodges, R. S., and Sykes, B. D. (1995) *J. Biomol. NMR 5*, 67−81.
37. Terzi, E., Hölzemann, G., and Seelig, J. (1995) *J. Mol. Biol. 252*, 633−642.
38. Snyder, S. W., Ladror, U. S., Wade, W. S., Wang, G. T., Barrett, L. W., Matayoshi, E. D., Huffake, H. J., Krafft, G. A., and Holzman, T. F. (1994) *Biophys. J. 67*, 1216−1228.
39. Durell, S. R., Guy, H. R., Arispe, N., Rojas, E., and Pollard, H. B. (1994) *Biophys. J. 67*, 2137−2145.
40. Schenck, H. L., Dado, G. P., and Gellman, S. H. (1996) *J. Am. Chem. Soc. 118*, 12487−12494.
41. Garcia-Echeverria, C. (1996) *Bioorg. Med. Chem. Lett. 6*, 229−232.

BI9810757